Characterization of a High-Power Fiber Master Oscillator Power Amplifier (MOPA) Laser as an Optical Communications Transmitter

M. W. Wright,[1] D. Zhu,[2] and W. Farr[1]

Deep-space optical communications requires high-power laser transmitters with good beam quality that can be modulated at fairly high data rates. We report here on the performance of a fiber-based master oscillator power amplifier (MOPA) laser, commercially developed to JPL requirements with specifications derived from a Mars mission optical downlink scenario. The laser demonstrates up to 1.6-kW peak power and an average power of around 10 W at 1060 nm with pulse repetition rates from 3 to 30 MHz and diffraction-limited beam quality. A programmable high-rate pulse-position modulator (PPM) also was developed as a data source, and the performance of the laser under variable pulse delays, as required for transmitting data streams, was measured.

I. Introduction

Fiber laser technology has seen significant development in recent years as a result of telecommunications and other commercial applications. The quest for higher powers in the remote sensing, marking and cutting, and medical communities means that fiber-based lasers now rival, and in some cases exceed, the performance of traditional solid-state laser systems. Free-space optical communications offers a unique convergence of industrial and telecommunication fields with the desire for high-power transmitters that can accommodate high modulation capabilities with good beam quality, as required at the large distances of interplanetary communication. Fiber-based lasers offer advantages for spaceborne applications, such as high efficiency, low volume, and mechanical robustness. Although output powers now routinely exceed 100 W [1–3] for continuous wave (CW) fiber lasers, pulsed systems that can operate at >1-MHz repetition rates with multikilowatt peak powers and multiwatt average powers are still in the development stage [4]. Obtaining high modulation quality of the output signal generally leads to master oscillator power amplifier (MOPA) geometries, where the device output modulation, linewidth, and wavelength are determined by the master or seed laser and the fiber amplifier raises the power to the required level. The seed laser can be either a direct-modulated diode laser or an externally modulated CW diode or fiber laser source. At the

[1] Communications Architectures and Research Section.

[2] Mobility and Robotic Systems Section.

The research described in this publication was carried out by the Jet Propulsion Laboratory, California Institute of Technology, under a contract with the National Aeronautics and Space Administration.

modest data rates of this downlink scenario, direct diode modulation is sufficient and involves less design complexity with lower cost. A near-future spaceborne optical communication demonstration is planned with the Mars Telecommunications Orbiter [5], and the preliminary link budget was used to baseline the performance specifications of the laser transmitter. Only a laboratory prototype was developed here, however, to demonstrate capability and to address performance issues when using pseudo-random pulse-position modulation (PPM) data streams.

II. Approach and Experiment

The fiber laser was developed by Keopsys, Inc., according to the requirements listed in Table 1. A schematic of the architecture is shown in Fig. 1, with the details of the construction given in [6] (in French). The components included a seed laser, consisting of a fiber Bragg grating (FBG) fiber-coupled

Table 1. Fiber laser specifications.

Parameter	Value	Verified
Average output power, P_{avg}	10 W	Yes
Repetition rate, PRF	3–30 MHz	Yes
Wavelength, λ_{CL}	<1064 nm	1060 nm
Linewidth, $\Delta\lambda$	<0.2 nm	0.02 nm
Peak power, P_p	1.67 kW at 3 MHz	Yes
Pulsewidth, τ	2 ns	1.8 ns
Beam quality, M^2	<1.2	Yes
Spatial mode	TEM_{00}	Yes
Wall plug efficiency (including thermo-electric cooler)	>5 percent	9 percent
Extinction ratio, ER (3–30 MHz)	>100 (20 dB)	21–47 dB
Polarization	Random	Yes
Energy stability (rms)	<5 percent	Yes
Pointing stability	< ±10 mrad	To be determined

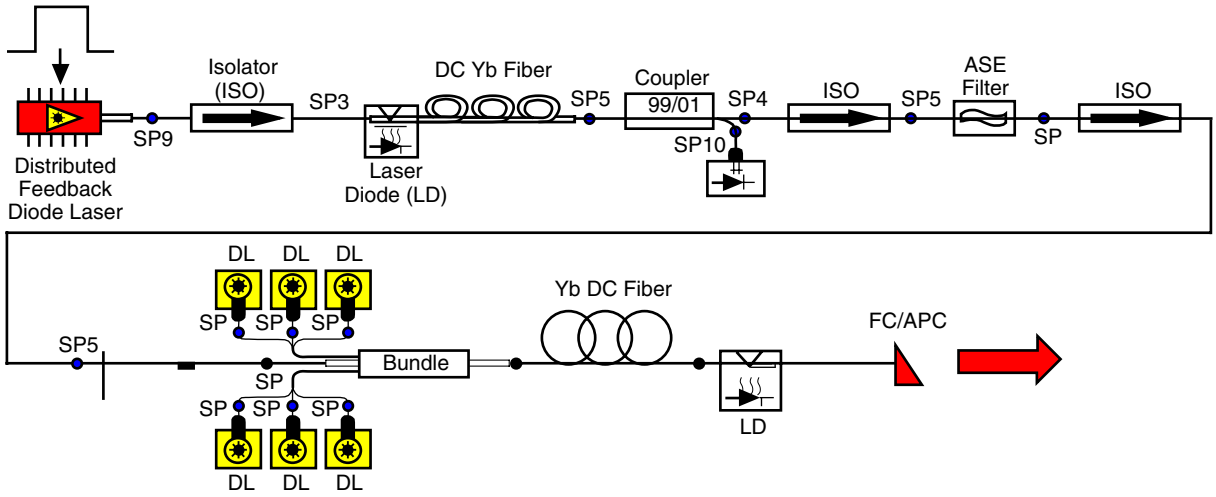

Fig. 1. Schematic of a fiber-based MOPA laser.

Fabry Perot (FP) laser diode at 1060 nm isolated from a dual-clad Yb-doped fiber preamplifier, followed by a Yb dual-clad fiber power amplifier. Each stage required filtering to limit the amount of amplified spontaneous emission propagated forward and isolation to avoid back oscillation. Several design iterations were explored by the vendor, including different fiber geometries and compositions to reach the desired performance level. The key elements were a suitably narrow linewidth source for the seed laser and a fiber design for the amplifier that could support the high peak powers. As the seed laser linewidth broadens during amplification, power is robbed from the central laser line. Other fiber nonlinearities such as four-wave mixing and self-phase-modulation also contribute to deplete the effective output power. The fiber geometry is critical since the appropriate length is required to produce enough gain, and the core diameter has to be sufficiently large to avoid Raman or stimulated Brillioun scattering while tailored via the index of refraction to maintain single-mode operation. Each stage was optimized separately, with the final power amplifier stage having a 13-μm core and 130×150-μm^2 clad fiber of 5-m length and approximately 2.5-dB/m pump absorption. Co-propagating diode laser pumps were utilized in a bundled-end pumped or V-groove side pumped approach with diodes at 920 or 975 nm. The output incorporated a fused 9-μm core diameter fiber coupled to a passive glass ferrule to allow for free beam expansion to limit the optical power density at the free-space boundary. A collimator was placed on the output to facilitate the measurements. The laser could be operated only in the pulsed mode.

Access to the output of the seed laser directly is not available in the integrated fiber laser, but a separate device from Lumics, Inc., identical to that used in the fiber MOPA system, was procured and tested in CW mode to determine the seed laser linewidth.

A PPM encoder based on a custom serializer circuit and a commercial off-the-shelf (COTS) field programmable gate array (FPGA) driver board was developed to produce pulse streams with variable delay simulating pseudo-random PPM-encoded bit streams. A block schematic is shown in Fig. 2. The board was designed to be driven entirely by the state machine code and the PPM data that are downloadable by the user. The encoder is completely flexible; different coding schemes can be accommodated by changing the state machine code. A Xilinx Virtex II (XC2V1500) FPGA stores the code (up to 64 kbytes) in its block random access memory (RAM), handles the user interface through the serial port, processes the state machine, and feeds data to the serializer board. The serializer board contains an 8-bit parallel-to-serial data converter that is a positive emitter-coupled logic (PECL) device capable of 3.2 Gb/s, and the converter sends a clock (PCLK) that is 1/8th of the serialization rate to the FPGA. The encoder also can accommodate fixed-pattern output without encoding.

The user programs the encoder through an asynchronous serial port. All commands are text based. The serial interface stores user-downloaded code to the block RAM. At each clock cycle, the FPGA reads the state machine code, decodes the code, and executes one or more of the following instructions: output a PPM code byte, shift in an on–off keying (OOK) bit, or reset. The FPGA sequentially steps through the state machine code memory until it reads a reset instruction, which causes it to start over. If the FPGA reads the shift instruction, the shift clock is enabled, and an OOK bit is clocked in to a holding buffer. The number of OOK bits clocked in determines the PPM order. If the FPGA reads the output instruction, the OOK bits in the holding buffer are converted to an address to the block RAM that contains the PPM code. Multiple output instructions cause the address to increment to accommodate the PPM code that extends multiple bytes. Since the PPM code is stored by the user, the OOK data can be mapped to any PPM format. For smaller-order PPM, a faster clock than the PCLK (1/8th PPM pulse rate) is needed. The FPGA's on-chip phase-locked loop (PLL) is used to generate clocks that are 4 times (for $2 \leq \text{PPM} \leq 8$) and 2 times (for $8 < \text{PPM} < 64$) the PCLK. After the state machine code is downloaded, the FPGA runs through the code once to determine the PPM order and chooses a clock automatically.

The emitter-coupled logic (ECL) output pulse from the serializer was converted to a transmitter–transmitter logic (TTL) level with a commercial pulse translator from Pulse Research Labs to interface

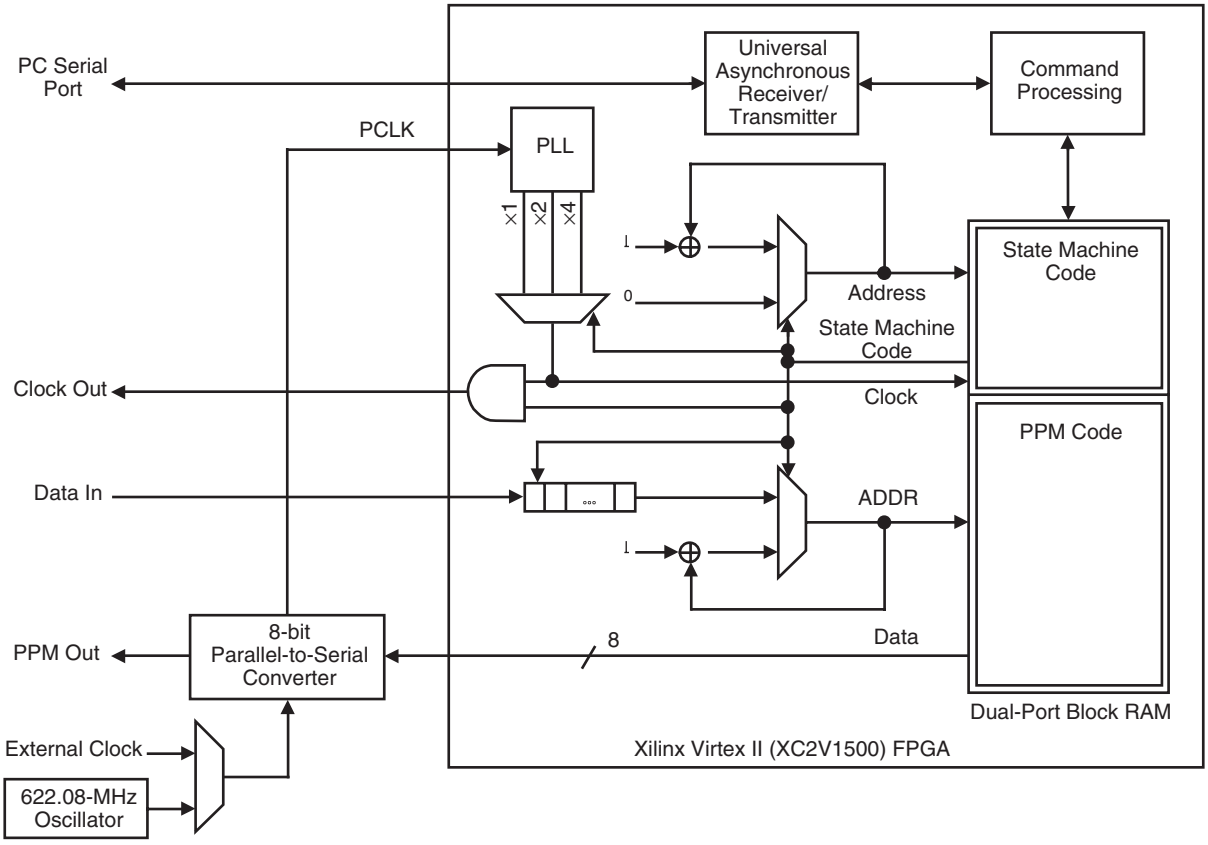

Fig. 2. Block diagram of the pseudo-PPM encoder.

to the laser drive electronics. Care had to be taken in choosing the various pulse delays to ensure they were within the range for the minimum and maximum pulse repetition frequencies (PRFs) of the fiber laser.

Average power measurements were made with a thermal power meter. Part of the signal from a beam splitter in the output beam was imaged into a 1×2 fiber-optic splitter so that simultaneous optical spectra and temporal pulse information could also be measured. The pulse detector was a Thorlabs InGaAs PIN diode with 1-GHz bandwidth, and the Ando optical spectrum analyzer (OSA) had a spectral resolution down to 0.01 nm. A Newport scanning FP meter with a free spectral range of 6 GHz was used for the stand-alone laser linewidth measurement of the seed laser. The output of the fiber laser could not be measured with the scanning FP meter because under pulsed operation the wavelength dithered or was broadened on the order of the free spectral range of the device. Based on the resolution of the OSA, an upper bound was determined from the spectral shape. The temporal pulse shapes were recorded on a 1.5-GHz Agilent digitizing oscilloscope. The extinction ratio or optical-signal-to-noise ratio (OSNR) also was taken from the optical spectra measurements. An 80-MHz Agilent high-speed pulser was used for fixed repetition rates and output TTL pulse shapes. Peak powers were derived by dividing the average power measurement with the PRF and the pulsewidth, assuming a near-square pulse shape, which is a reasonable approximation for our pulses.

III. Results

The output power as a function of amplifier drive current is shown in Fig. 3 for several fixed repetition rates. To avoid reducing the operational life of the system, the current was limited to 4.5 A, slightly below the maximum specified to obtain 10 W. Figure 4 depicts the log optical spectra at 3 and 30 MHz. It can be seen that the laser line is on the high energy side of the gain or amplified spontaneous emission (ASE) peak centered at 1080 nm, with the weak presence of fiber nonlinearities [7] around 1115 nm on the high peak power region at low PRF. Taking linear optical spectra (Fig. 5), allow the full-width half-maximum (FWHM) linewidth to be measured at varying output power levels. The resolution limit on the spectrum analyzer sets an upper limit for the linewidth with the appearance of the single longitudinal mode. It was observed that, with repeated measurements over a period of several days, the central peak broadened from 0.01 nm, the resolution of the OSA, to the currently plotted values of around 0.02 to 0.05 nm.

In order to receive the weak signal from a deep-space laser transmitter in the presence of strong background light, a narrowband optical filter would be employed in the receiver system to enhance the optical-signal-to-noise ratio. Typical downlink linewidths have been specified on the order of the subnanometer level [5]; hence, the power within a 1-Å bandwidth was measured for the various spectra and tabulated in Table 2 along with the measured FWHM linewidths, $\Delta\lambda$.

The CW equivalent linewidth of the seed laser is shown in Fig. 6 and typically had a value of 24 MHz.

A representative temporal pulse shape is shown in Fig. 7 with an FWHM of 1.7 ns. The dual peaks were always present, but their exact origin is uncertain.

The PPM encoder was also used as the input signal to drive the laser with variable pulse delays within the constraints of the 3- (333-ns pulse delay) to 30-MHz (33-ns) PRF. These data streams are shown in Fig. 8, with the corresponding output spectra shown in Fig. 9. The device had to reach thermal equilibrium at the higher operating currents; otherwise, multimode operation was evident. The center wavelengths and linewidths also were measured and are shown in Table 2.

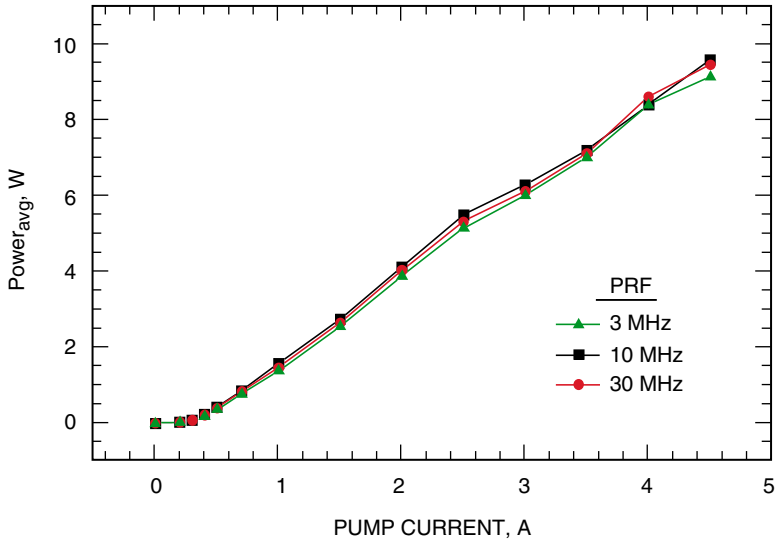

Fig. 3. Average output power versus pump current for various fixed PRFs.

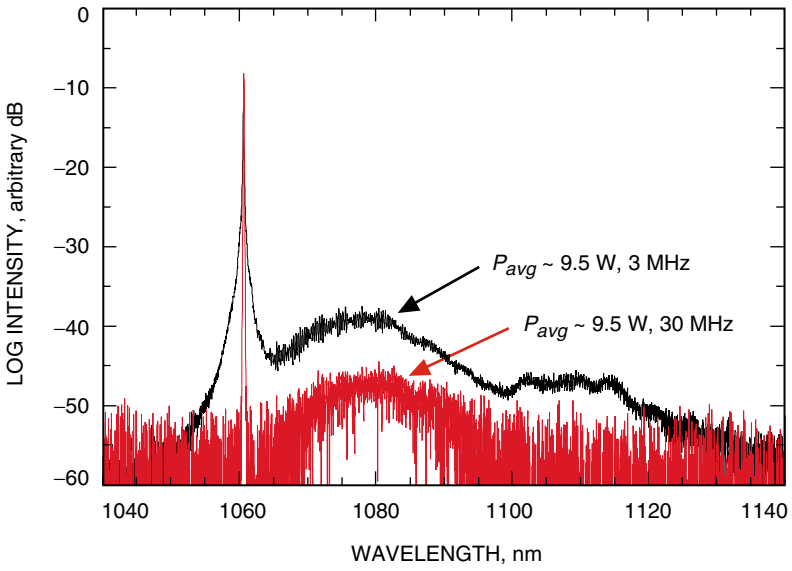

Fig. 4. Optical spectra for 3- and 30-MHz PRFs at near-maximum output power.

The pulse-to-pulse stability of the output was monitored under variable repetition rates. As the pulse delay was decreased from the fixed rate of 3 MHz, the following pulse experienced a slight decrease in amplitude but still was within the 1 to 2 percent repeatability. However, when the pulse delay corresponded to switching the repetition rate from 30 to 3 MHz, as shown in Fig. 8, the following peak pulse height was reduced on average by 6.5 percent, suggesting there is some PRF dependence in the pulse energy in this extreme condition, as expected from gain depletion.

The OSNR was taken from the optical spectra by measuring the laser line peak to the signal ±0.5 nm from the peak wavelength at over 9-W output power. The values ranged from 21 dB at 3 MHz to 47 dB at 30 MHz. When the device was switched between 3 and 30 MHz, an OSNR of 23 dB was observed at maximum output power. The laser line peak may be compared to the broad ASE peak; this measurement would add a few decibels to the OSNR. It would appear that this PRF range can be extended; nonlinearities do not yet dominate the optical spectra. Future work will investigate the operational limits of this device, but for the present work we operated within the manufacturer's specified region.

The beam quality was measured by the manufacturer and gave an $M^2 < 1.2$ and is consistent with the output being a single-mode fiber coupled to a passive glass ferrule [4]. The wall plug efficiency was given as 9 percent or 11.3 percent if only the DC efficiency is used, both including thermal management. The output beam was not polarized; however, polarization-maintaining fiber could be incorporated in a future amplifier design.

Finally, it was noted that, while maintaining high average output power, there was a 5 to 10 percent drop in the power level over approximately 30 to 40 minutes. This was recoverable once the device was switched off and on again, suggesting some thermal effects, possibly detuning of the pump laser wavelengths with time. Ongoing life tests will be investigated further in a future article.

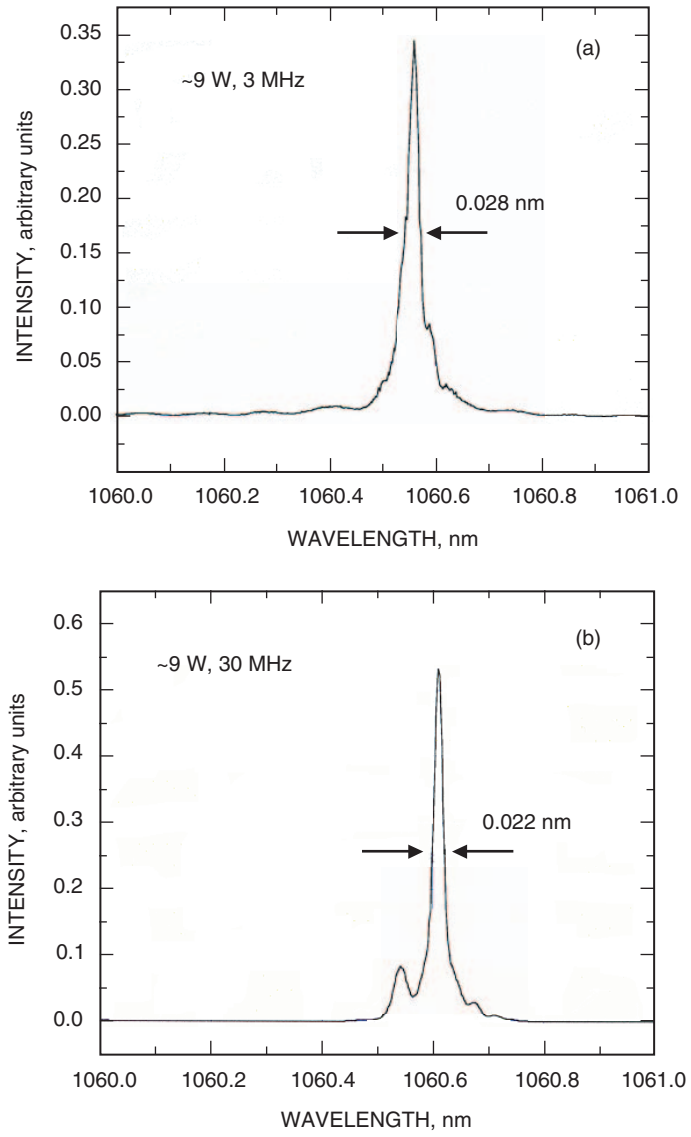

Fig. 5. High-resolution spectra for two fixed PRFs, showing the narrow linewidth: (a) 3 MHz and (b) 30 MHz.

IV. Discussion

The pulsed fiber laser met the design requirements and, in some cases, such as the linewidth and efficiency, exceeded them significantly. The development required several iterations in the choice of fiber for the amplifier stage and in obtaining a suitably narrow seed laser source around 1064 nm. A broadened seed laser linewidth limited the peak power obtainable through amplification, requiring longer fiber lengths to increase the gain, with the associated rise in the nonlinear effects. On the other hand, increasing the fiber core diameter to mitigate the nonlinear effects required increased pump levels and decreased the overall efficiency. Self-phase-modulation also increased the laser linewidth for certain amplifier geometries, even when a narrow linewidth source was implemented. The fiber composition had to be specifically tailored to balance the competing gain and linewidth requirements.

Table 2. Pulsed performance at fixed PRFs and at the extreme of pulse delays (3+30 MHz).

PRF, MHz	P_{avg}, W	P_{peak}, W	τ_{pulse}, ns	Energy, μJ/pulse	$\Delta\lambda$, nm	P, $\Delta\lambda = 1$ Å, percent
3	9.2	1500	1.91	3	0.028	71
5	9.5[a]	860	2.0	1.7	0.048	70
10	9.6	480	2.04	0.96	∼0.02[a]	∼70[a]
30	9.5	135	2.35	0.32	0.022	80
3 + 30	9.5	870	2.04	1.7	0.028	77

[a] Scaled from preliminary measurements.

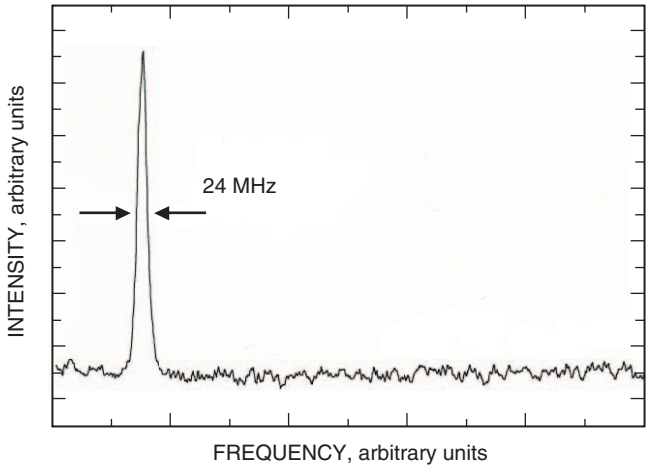

Fig. 6. Scanning the Fabry–Perot spectrum of a CW oscillator laser.

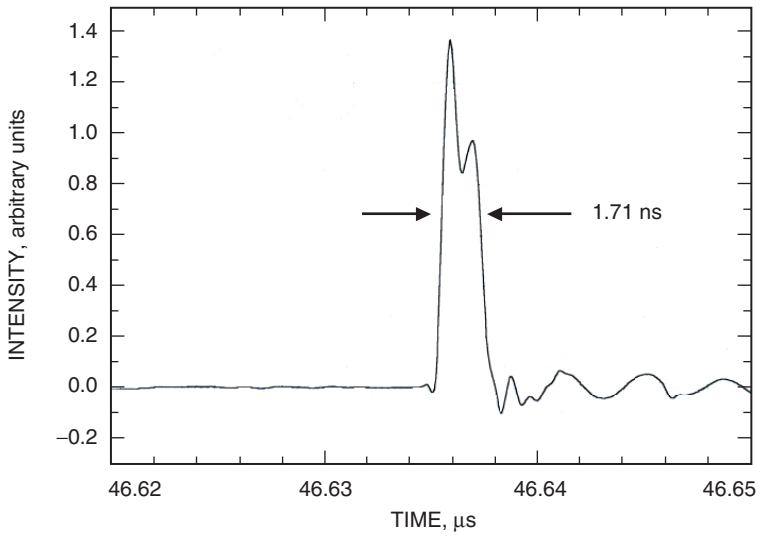

Fig. 7. Temporal pulse shape of the output signal for 3-MHz, 9-W average power.

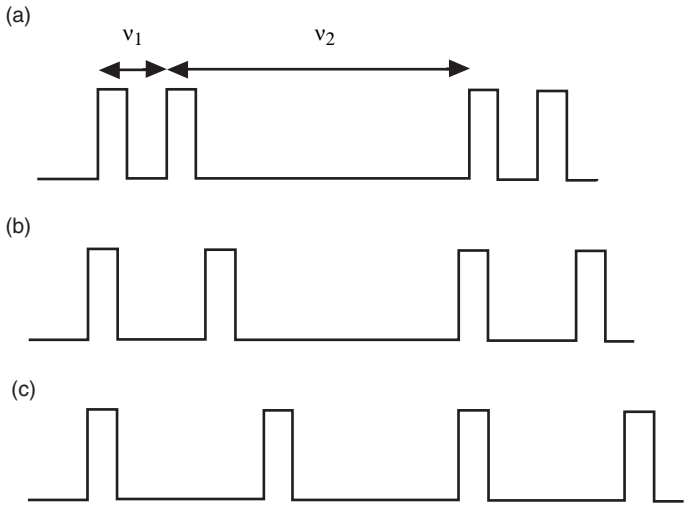

Fig. 8. Data patterns input to the PPM encoder, corresponding to (a) ν_1, ν_2 = 30, 3 MHz or Δt = 33, 333 ns; **(b)** ν_1, ν_2 = 9.2, 3.8 MHz or Δt = 109, 259 ns; and **(c)** ν_1, ν_2 = 6.8, 4.5 MHz or Δt = 147, 220 ns.

Along with the laser linewidth, the center line value of the output is a critical parameter for the optical downlink. Narrow linewidth is required to enable background light rejection, improving the signal-to-noise ratio of the received signal, as noted above. Any spectral filtering must encompass the entire pulse repetition frequency region of operation and, hence, the center wavelength must be stable with respect to the filter bandwidth to minimize any detuning in the optical receiver. It is interesting to note that, apart from the fixed 30-MHz PRF case, the laser center frequencies are within 0.008 nm of each other. The broadening over time may result from either thermal detuning of the pump wavelength limiting the power output or some degradation due to nonlinear effects. Ongoing life tests currently are being performed.

It is worth comparing the performance of the laser under pseudo-random PPM with that under fixed PRF. Maintaining the 10-W average output power with fixed pump input power and the same pulsewidth over the entire PRFs, the peak power varies from around 1.6 kW at 3 MHz to 160 W at 30 MHz. The pulse shape over the PRF range was consistent, as seen in Fig 10. When used as a data transmitter with PPM, the delay between pulses varies and, hence, one would expect the peak power or pulse energy to vary significantly as well. Figure 8 simulates this most demanding case, with the data switched from a 3- to 30-MHz PRF (or, equivalently, a pulse separation of 30 to 330 ns). It would appear that pulsing the laser at variable data rates does not significantly reduce the pulse energy, with only a weak PRF dependence. The amplifier gain is able to support a single pulse within the pulse delay imposed by the PRF requirements. This is how the device would operate as a PPM transmitter. In order to produce the reduced peak powers at the higher PRFs, a much longer pulse stream of fixed pulse delays is required, which does not occur with high rate.

V. Conclusion

A fiber MOPA laser was designed to satisfy a Mars mission downlink scenario and was successfully developed through a commercial vendor. It demonstrated high, near 10-W, average power under pulsed operation and could transmit random data streams from 3 to 30 MHz at up to 1.6-kW peak power in sub-2-ns pulses. A custom PPM encoder was built and integrated with the laser to represent a prototype transmitter for deep-space optical communications.

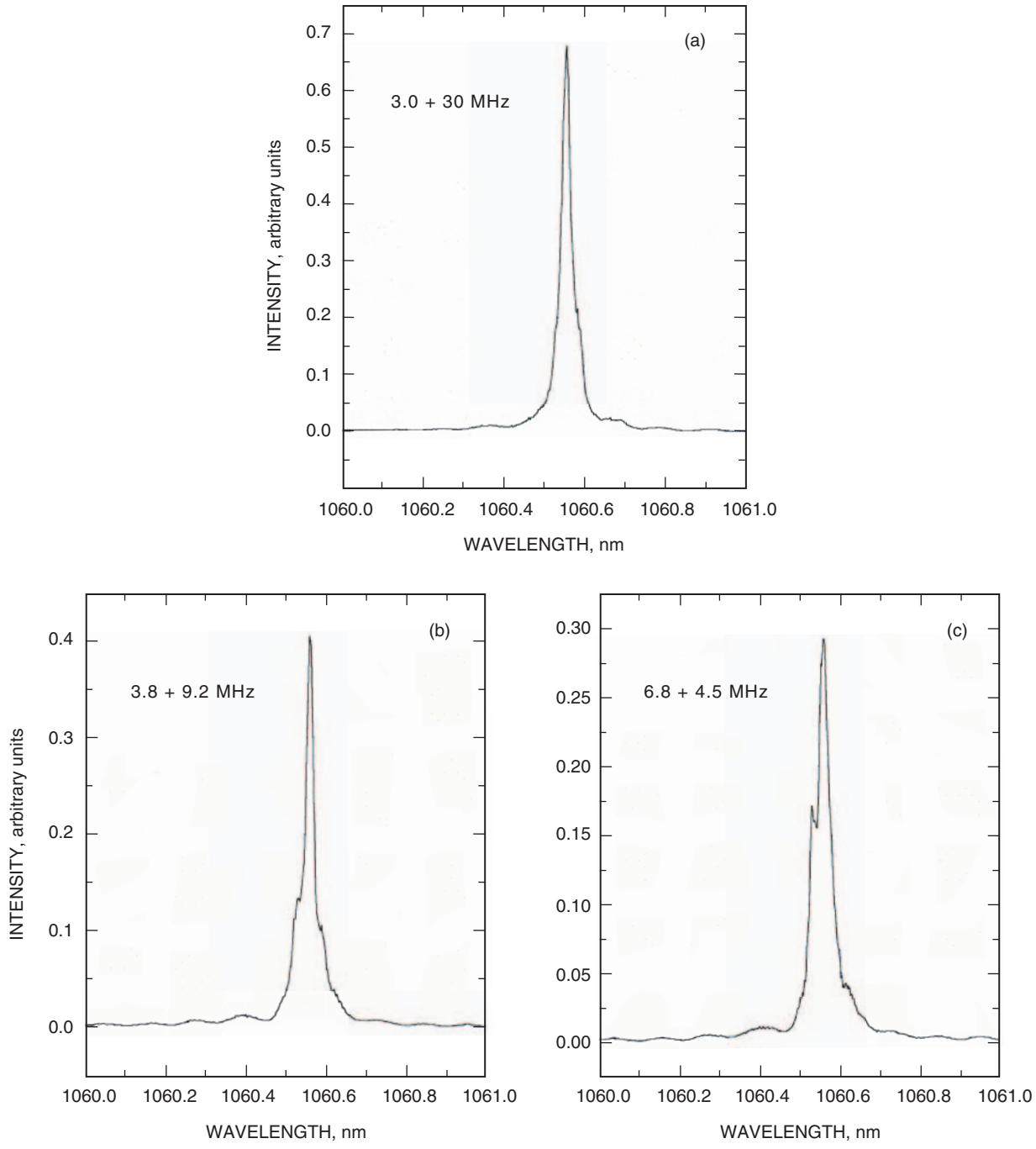

Fig. 9. High-resolution spectra for signal inputs corresponding to conditions (a), (b), and (c) of Fig. 8.

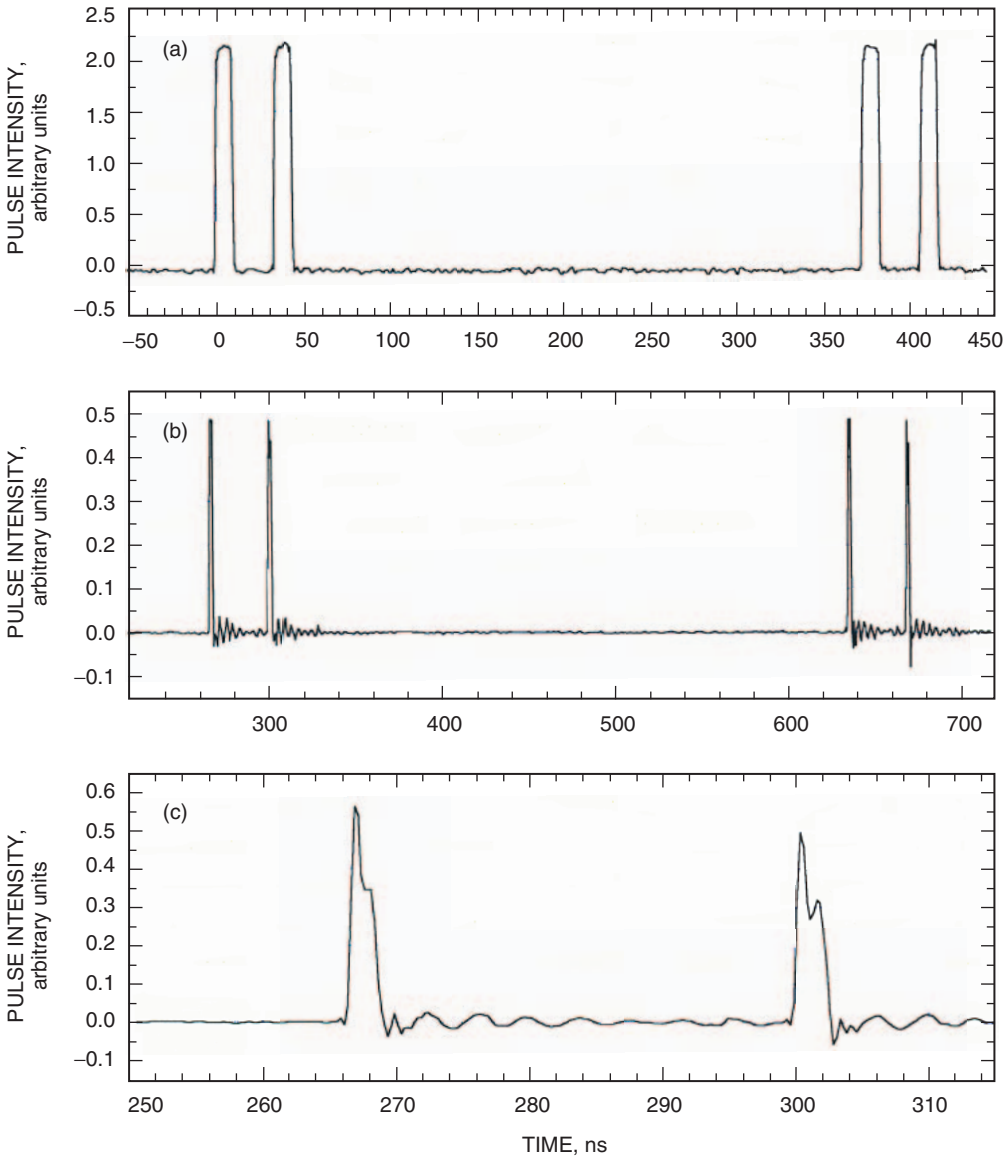

Fig. 10. Temporal pulse streams: (a) RF pulse from the pseudo-PPM encoder output at 3 + 30 MHz, (b) output of the fiber MOPA at approximately 9-W average power, and (c) an expanded time scale of (b).

References

[1] D. Gapontsev, "Recent Progress on High Power Fiber Lasers," *Diode and Solid State Laser Technology Rev.*, Albuquerque, New Mexico, June 2004.

[2] J. Jeong, J. K. Sahu, D. N. Payne, and J. Nilsson, "Yb Doped Large Core Fiber Laser with 1 kW CW Output Power," *Advanced Solid State Photonics*, Santa Fe, New Mexico, February 2004.

[3] A. Galvanauskas and B. Samson, "High Fiber," *OEmagazine*, pp. 15–17, July 2004.

[4] P. A. Champert, S. V. Popov, M. A. Solodyankin, and J. R. Taylor, "Multiwatt Average Power Continua Generation in Holey Fibers Pumped by kW Peak Power Seeded Yb Fiber Amplifier," *Appl. Phys. Lett.*, vol. 81 no. 12, pp. 2157–2159, 2002.

[5] S. A. Townes, B. L. Edwards, A. Biswas, D. R. Bold, R. S. Bondurant, D. Boroson, J. W. Burnside, D. O. Caplan, A. E. DeCew, R. DePaula, R. S. Fitzgerald, F. I. Khatri, A. K. McIntosh, O. V. Murphy, B. A. Parvin, A. D. Pillsbury, W. T. Roberts, J. J. Scozzafava, J. Sharma, and M. Wright, "Ground System of the Mars LaserComm Demonstration," IEEE Aerospace, Big Sky, Montana, March 2004.

[6] S. Grot, L. Goldberg, P. Besnard, and Y. Jaouen, "Generation d'Impulsions Mochromatiques Breves au-dela de 1.7 kW par Amplification a Fibre Dopee Yb," *23emes Journées Nationales d'Optique Guidée*, Paris, France, October 2004.

[7] E. Desurvire, *Erbium Doped Fiber Amplifiers*, New York: John Wiley and Sons, 1994.